HEPATOLOGY

HEPATOLOGY, VOL. 69, NO. 2, 2019

DDX24 Mutations Associated With Malformations of Major Vessels to the Viscera

Pengfei Pang,[1-3*] Xiaojun Hu,[1-3*] Bin Zhou,[1-3*] Junjie Mao,[1-3*] Yu Liang,[4] Zaibo Jiang,[5] Mingsheng Huang,[5] Ruihong Liu,[2] Youyong Zhang,[5] Jiesheng Qian,[5] Jinsong Liu,[6] Jinxin Xu,[6] Yaqin Zhang,[2] Maoheng Zu,[7] Yiming Wang,[2-4**] Huanhuan He,[2**] and Hong Shan[1-3**]

Vascular malformations present diagnostic and treatment challenges. In particular, malformations of vessels to the viscera are often diagnosed late or incorrectly due to the insidious onset and deep location of the disease. Therefore, a better knowledge of the genetic mutations underlying such diseases is needed. Here, we evaluated a four-generation family carrying vascular malformations of major vessels that affect multiple organs, which we named "multiorgan venous and lymphatic defect" (MOVLD) syndrome. Genetic analyses identified an association between a mutation in DEAD-box helicase 24 (*DDX24*), a gene for which the function is largely unknown, and MOVLD. Next, we screened 161 patients with sporadic vascular malformations of similar phenotype to our MOVLD family and found the same mutation or one of the two additional *DDX24* mutations in 26 cases. Structural modeling revealed that two of the mutations are located within the adenosine triphosphate–binding domain of DDX24. Knockdown of *DDX24* expression in endothelial cells resulted in elevated migration and tube formation. Transcriptomic analysis linked *DDX24* to vascular system–related functions. *Conclusion*: Our results provide a link between DDX24 and vascular malformation and indicate a crucial role for DDX24 in endothelial cell functions; these findings create an opportunity for genetic diagnosis and therapeutic targeting of malformations of vessels to the viscera. (Hepatology 2019;69:803-816).

Vascular malformations are present in approximately 1.5% of the general population.[1,2] The majority of reported vascular malformations involve the head, neck, trunk surface, and extremities. As these locations are conspicuous, patients with these diseases tend to receive timely diagnosis and treatment. In contrast, patients with malformations of vessels in or to the viscera generally come to medical attention only when severe complications occur, due to the insidious onset and deep location of the disease. This can lead to a delay in diagnosis and treatment or, in some cases, missed or incorrect diagnoses.[3-6] Therefore, vascular malformations may not be as rare as they are thought to be, and understanding their genetics and pathogenesis will contribute to the diagnosis and treatment of the diseases.

Abbreviations: ACMG, American College of Medical Genetics and Genomics; ATP, adenosine triphosphate; BCS, Budd-Chiari syndrome; CT, computed tomography; CX3CR1, C-X3-C motif chemokine receptor 1; DDX24, DEAD-box helicase 24; ExLOD, exponential logarithm of the odds; HHSEC, human hepatic sinusoidal endothelial cell; HLEC, human lymphatic endothelial cell; HUVEC, human umbilical vein endothelial cell; ISSVA, International Society for the Study of Vascular Anomalies; MIM, Mendelian Inheritance in Man; MOVLD, multiorgan venous and lymphatic defect syndrome; PDB, Protein Data Bank; PTAFR, platelet-activating factor receptor; siRNA, small interfering RNA; SNP, single-nucleotide polymorphism.

Received May 27, 2018; accepted July 26, 2018.

Additional Supporting Information may be found at onlinelibrary.wiley.com/doi/10.1002/hep.30200/suppinfo.

**These first authors contributed equally to this work.*

***These senior authors contributed equally to this work.*

Supported by grants from the National Natural Science Foundation of China (31741068, 81430041, 81620108017, and 81501561), the Science and Technology Planning Project of Guangzhou Province (201604020098 and 201610010006), the Natural Science Foundation of Guangdong Province (2014A030310043 and 2017A030313873), the High Level Health Care Team of Zhuhai City (33010102020703), the High Level Health Care Individual of Zhuhai City (33010102020701), the High Level Clinical Key Specialty Project of Zhuhai City (33010102020605), and the Outstanding Talent Program of Guangdong Province (Nan Yue Bai Jie).

Genetic mutations are known to play an important role in vascular malformations.[7-11] For example, mutations of the TEK receptor tyrosine kinase and glomulin genes have been associated with venous malformations (Mendelian Inheritance in Man [MIM] 600195 and 138000),[12,13] and mutated Fms-related tyrosine kinase 4 is considered to be the causal gene of certain types of lymphatic malformations (MIM 153100).[14] In addition, mutations of RAS p21 protein activator 1, ephrin receptor B4, and Krev interaction trapped 1 are found in mixed vascular malformations (MIM 608354 and 116860).[15-18] However, the causal genes have been associated rarely with malformations of vessels to the viscera.

To gain insight into the underlying causes of malformations of vessels to the viscera, we evaluated a four-generation family carrying vascular malformations affecting multiple organs with stenosis or occlusion of portal and hepatic veins and/or lymphatic vessels, as well as formation of collateral circulation and pulmonary valve stenosis, resulting in portal hypertension, chylothorax, edema of the lower extremities, and pulmonary hypertension. We named this condition "multiorgan venous and lymphatic defect" (MOVLD) syndrome. The phenotypes segregated in the family in an autosomal dominant fashion. We aimed to determine the genetic basis of this syndrome and 161 sporadic cases with similar phenotype and to provide insight into the pathogenetic basis of malformations of vessels to the viscera, which will be valuable in aiding the future diagnosis and treatment of patients with similar diseases.

View this article online at wileyonlinelibrary.com.
DOI 10.1002/hep.30200

Potential conflict of interest: Nothing to report.

ARTICLE INFORMATION:

From the [1]Department of Interventional Medicine; [2]Guangdong Provincial Engineering Research Center of Molecular Imaging, The Fifth Affiliated Hospital, Sun Yat-sen University; [3]Institute of Interventional Radiology, Sun Yat-sen University, Zhuhai, China; [4]BGI-Shenzhen, Shenzhen, China; [5]Department of Interventional Medicine, The Third Affiliated Hospital, Sun Yat-sen University, Guangzhou, China; [6]State Key Laboratory of Respiratory Disease, Guangzhou Institutes of Biomedicine and Health, Chinese Academy of Sciences, Guangzhou, China; [7]Department of Interventional Radiology, The Affiliated Hospital of Xuzhou Medical College, Xuzhou, China.

ADDRESS CORRESPONDENCE AND REPRINT REQUESTS TO:

Hong Shan, M.D.
Department of Interventional Medicine
The Fifth Affiliated Hospital
Sun Yat-sen University
Zhuhai, China
E-mail: shanhong@mail.sysu.edu.cn
Tel: +86756-2528947
or
Huanhuan He, Ph.D.
Guangdong Provincial Engineering
Research Center of Molecular Imaging
The Fifth Affiliated Hospital
Sun Yat-sen University
Zhuhai, China
E-mail: hehh23@mail.sysu.edu.cn
Tel: +86756-2526143
or
Yiming Wang, Ph.D.
Guangdong Provincial Engineering
Research Center of Molecular Imaging
The Fifth Affiliated Hospital
Sun Yat-sen University
Zhuhai, China
E-mail: ywzhong@hotmail.com
Tel: +86756-2526143
or
Maoheng Zu, M.D.
Department of Interventional Radiology
The Affiliated Hospital of Xuzhou Medical College
Xuzhou, China
E-mail: zumaoheng@163.com
Tel: +86516-85802116
or
Youyong Zhang
Department of Interventional Medicine
Yuebei People's Hospital
Shaoguan, China
E-mail: 244390627@qq.com

Materials and Methods

PATIENTS

The proband of the family was referred to us from Puyang, China, due to refractory chylothorax. After clinical investigation of the proband, we collected clinical information for all members in the family, which comprises 51 members, spanning four generations, with 10 affected members, including 8 who were alive and available for the study. The information of family member I-1 was unavailable. We also studied the medical records, including the imaging records, of the two affected deceased family members (II-4 and III-16). All participants were of Chinese Han ethnicity. Written informed consent was obtained. The study was approved by the Ethics Committee of The Fifth Affiliated Hospital, Sun Yat-sen University. Principles of the Declaration of Helsinki were followed.

CLINICAL EVALUATION

Imaging characteristics were evaluated using computed tomography (CT; for individuals who were ≥13 years of age at the time of enrollment) or ultrasonography (for individuals who were <13 years of age at the time of enrollment) by three independent imaging specialists. A liver biopsy was performed in 3 affected members (II-6, III-8, and III-15). We then assessed for all possible causes of the syndrome in the family such as hepatitis, autoimmune diseases, vasculitis, coagulation disorders, or history of abdominal surgery and trauma.[19,20] Routine blood tests were done to exclude the possibility of infection in all sporadic cases. The absence of antinuclear antibody and rheumatoid factor in all of the patients precluded the possibility of autoimmune disease. Laboratory investigation confirmed normal kidney, liver, and blood coagulation functions. According to medical history and physical examination, none of the patients had newborn omphalitis, trauma, or other physical illness.

GENETIC ANALYSIS

Chromosome microarray analysis using Agilent CytoGenomics software (version 3.0; https://www.genomics.agilent.com/) was performed using DNA samples of family members II-8, II-10, II-12, and III-15 to investigate if changes at the chromosome level were responsible for the disease phenotypes. Data were analyzed using Online MIM (https://omim.org/), UniGene (https://www.ncbi.nlm.nih.gov/unigene), the Conserved Domain Database (https://www.ncbi.nlm.nih.gov/Structure/cdd/cdd.shtml), BioGPS (https://biogps.org/), and the Database of Genomic Variants 14 (https://dgv.tcag.ca/dgv/app/home). Polymorphic copy number variations already reported in the Database of Genomic Variants 14 and known to be benign were excluded from further consideration.

Genomic DNA was extracted from peripheral blood of 16 adults from the second and third generations of the family using the standard protocols (Qiagen, Germany) and genotyped using SNP Array 6.0 (Affymetrix), which covers 908,476 single-nucleotide polymorphism (SNP) markers. Exponential logarithm of the odds (ExLOD) scores were calculated from the Kong and Cox exponential model using MERLIN 1.1.2.2.[21] I-2, II-3, II-5, II-6, II-8, II-9, II-10, II-12, II-14, III-8, III-10, III-12, III-13, III-15, III-18, and III-19 were recruited for linkage analysis, which identified three candidate regions that had ExLOD scores >3.0. Within these regions, one SNP out of every five was selected as a tag SNP, and haplotypes were constructed using HaploPainter.[22] Haplotype cosegregation analysis identified a single haplotype which cosegregated with the disease phenotype and was on the highest ExLOD locus 14q32.12 flanked by markers rs4900162 and rs8006174.

Exome sequencing was performed in 2 affected (III-8 and III-10) and 2 unaffected (II-8 and II-12) members, who we fully evaluated (see above, Clinical Evaluation) and excluded for all possible symptoms of MOVLD, using Illumina Hiseq 2000 with a paired-end 100-bp length configuration (GSA #CRA000816). High-quality reads were mapped against the human reference genome (hg1.9) from the University of California Santa Cruz Genome Browser (https://genome.ucsc.edu/) using the Burrows-Wheeler Aligner program.[23] SNPs were identified using SOAP snp (version 0.1.19; https://sourceforge.net/projects/soapsnp/files/soapsnp/download), and small insertions/deletions were identified by Samtools.[24] ANNOVAR was used for variant annotation.[25] All variations predicted to be deleterious by Polyphen-2 (http://genetics.bwh.harvard.edu/pph2/) and shared by the 2 affected individuals but absent

in the 2 unaffected family members were classified using the American College of Medical Genetics and Genomics (ACMG) guidelines.[26] Sanger sequencing (primer sequences are provided in Supporting Table S1) was used in all family members available for genetic analysis to confirm that the mutations were shared by all of the affected but absent in the remaining family members available for genetic analysis. One hundred control samples were collected from people who underwent clinical and imaging examinations and appeared normal.

SPORADIC PATIENT RECRUITMENT

To further investigate the involvement of the putative causative gene from this family in unrelated patients with similar vascular features, we recruited 10 patients exhibiting portal vein stenosis or occlusion with formation of collateral circulation as well as 151 idiopathic Budd-Chiari syndrome (BCS) patients characterized by stenosis or occlusion of the hepatic vein and/or inferior vena cava.[27,28] And according to the location of obstruction, the BCS cases were classified as three types: pure obstruction of hepatic vein, pure obstruction of inferior vena cava, combined obstruction of hepatic vein and inferior vena cava (Table 1).[29] All of the known causes of vascular malformations (including hepatitis, autoimmune diseases, vasculitis, coagulation disorders, and history of abdominal surgery and trauma) were excluded in all 161 patients (for details, see above, Clinical Evaluation). All sporadic cases had a healthy diet and did not have any history of serious health problems. For all patients, PCR and Sanger sequencing were performed in the exons and intron–exon boundaries of the causative gene in genomic DNA extracted from blood.

STRUCTURAL MODEL BUILDING

The structure of the protein encoded by the causative gene was modeled using Discovery studio 3.5 (BIOVIA). The crystal structure of the N-terminal domain of HERA (Protein Data Bank [PDB] 2GXQ) was used as a template for homology modeling.[30] MODELER was used to validate the model of the causative protein.[31]

1.6. FUNCTIONAL ASSAYS

To detect the vascular system–related functions of the causative protein, two small interfering RNAs (siRNAs; sequences are provided in Supporting Table S2) targeting the causative gene were designed using GenScript bioinformatics tools (https://www.genscript.com/tools/sirna-target-finder) and transfected into human umbilical vein endothelial cells (HUVECs; Sciencell), human lymphatic endothelial cells (HLECs; Sciencell), and human hepatic sinusoidal endothelial cells (HHSECs; Sciencell) using Lipofectamine 3000 (Invitrogen) with scrambled siRNA (RIBOBIO, China) as negative control. The knockdown efficiency was determined by reverse-transcription real-time quantitative PCR and western blotting (additional details can be found in the Supporting Information). Cellular viability was evaluated using a Cell Counting Kit-8 (Dojinbo, Japan). Cell migration was examined using a modified Boyden chamber assay with 24-well chambers (BD).[32] A tube formation assay was performed as described.[33] RNA sequencing analysis was performed on siRNA-targeted HUVECs and control HUVECs to evaluate the effects of the causative gene knockdown on expression of other genes (GSE #117133, additional details can be found in the Supporting Information). Genes were randomly selected for real-time quantitative PCR to validate the RNA sequencing results, and genes involved in cell migration were identified by reverse-transcription real-time quantitative PCR. The methods of cellular function assays are described in detail in the Supporting Information.

Results

MOVLD PATIENT CHARACTERISTICS

We evaluated a four-generation family with vascular malformations involving multiple organs. Ten affected members in this large family, including 8 alive and 2 deceased, exhibited stenosis or occlusion of portal and hepatic veins (Fig. 1 and Table 1), with various additional clinical presentations including thoracic duct obliteration, pulmonary valve stenosis, and other thoracoabdominal vascular lesions (Fig. 2; Supporting Figs. S1-S7). Out of the 10 affected members, III-15,

TABLE 1. Clinical Characteristics of the Patients and their *DDX24* Mutations

Patient	Sex	Age at diagnosis (years)	Clinical characteristics	Mutation
Patients from the MOVLD syndrome family				
II-4	F	43	Portal vein occlusion, hepatic vein stenosis, thoracic duct obliteration, pulmonary valve stenosis, splenomegaly, oesophageal varices	ND
II-6	F	50	Portal vein stenosis, hepatic vein stenosis, thoracic duct obliteration, splenomegaly, oesophageal varices, portal cavernoma	p.Glu271Lys
II-10	F	44	Portal vein occlusion, hepatic vein stenosis, thoracic duct obliteration, ascites, pericardial effusion, splenomegaly, oesophageal varices	p.Glu271Lys
III-8	F	36	Portal vein occlusion, hepatic vein stenosis, splenomegaly, oesophageal varices, fundus varication, gastro-renal shunt	p.Glu271Lys
III-10	F	31	Portal vein occlusion, hepatic vein stenosis, splenomegaly, oesophageal varices	p.Glu271Lys
III-12	F	28	Portal vein occlusion, hepatic vein stenosis, thoracic duct obliteration, pericardial effusion, splenomegaly, oesophageal varices, fundus varication	p.Glu271Lys
III-13	M	27	Portal vein occlusion, hepatic vein stenosis, pulmonary valve stenosis, splenomegaly	p.Glu271Lys
III-15	F	16	Portal vein stenosis, hepatic vein stenosis, thoracic duct obliteration, ascites, pericardial effusion, oesophageal varices, fundus varication	p.Glu271Lys
III-16	M	14	Portal vein occlusion, hepatic vein stenosis, thoracic duct obliteration, splenomegaly, oesophageal varices	ND
IV-10	M	5	pulmonary valve stenosis	p.Glu271Lys
Sporadic Patient with portal vein lesion*				
GD01	M	43	Portal vein stenosis with formation of collateral circulation	p.Glu271Lys
Patients with idiopathic Budd-Chiari syndrome#				
XZ012	F	32	Pure obstruction of hepatic vein	p.Glu271Lys
XZ015	M	46	Pure obstruction of inferior vena cava	p.Glu271Lys
XZ022	F	38	Pure obstruction of hepatic vein	p.Glu271Lys
XZ028	M	43	Pure obstruction of inferior vena cava	p.Glu271Lys
XZ030	M	50	Pure obstruction of inferior vena cava	p.Glu271Lys
XZ049	F	60	Combined obstcution of hepatic vein and inferior vena cava	p.Glu271Lys
XZ052	M	30	Pure obstruction of inferior vena cava	p.Glu271Lys
XZ057	M	21	Pure obstruction of hepatic vein	p.Glu271Lys
XZ061	M	24	Combined obstcution of hepatic vein and inferior vena cava	p.Glu271Lys
XZ062	F	47	Pure obstruction of inferior vena cava	p.Glu271Lys
XZ066	F	29	Pure obstruction of hepatic vein	p.Glu271Lys
XZ069	M	50	Pure obstruction of inferior vena cava	p.Glu271Lys
XZ101	M	65	Pure obstruction of inferior vena cava	p.Glu271Lys
XZ100	M	31	Pure obstruction of hepatic vein	p.Glu271Lys
XZ003	F	23	Pure obstruction of hepatic vein	p.Lys11Glu
XZ004	F	45	Pure obstruction of hepatic vein	p.Lys11Glu
XZ106	F	45	Pure obstruction of inferior vena cava	p.Lys11Glu
XZ110	M	37	Pure obstruction of inferior vena cava	p.Lys11Glu
XZ113	M	60	Pure obstruction of inferior vena cava	p.Lys11Glu
XZ122	F	76	Pure obstruction of inferior vena cava	p.Lys11Glu
XZ130	M	21	Pure obstruction of hepatic vein	p.Lys11Glu
XZ132	F	60	Pure obstruction of inferior vena cava	p.Lys11Glu
XZ136	F	63	Pure obstruction of inferior vena cava	p.Lys11Glu
XZ142	F	39	Pure obstruction of hepatic vein	p.Lys11Glu
XZ103	F	41	Combined obstcution of hepatic vein and inferior vena cava	p.Arg436His

F: female; M: male; ND: no data.
*All the known causes of portal vein lesion were excluded.
#Budd-Chiari syndrome classification according to the location of obstruction.

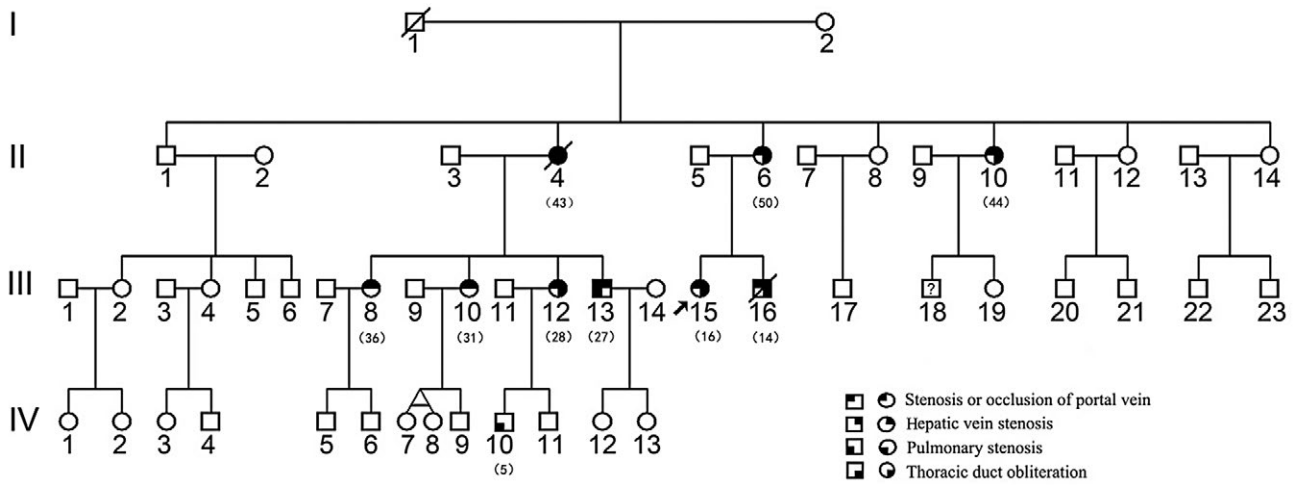

FIG. 1. Pedigree of the family with MOVLD syndrome. The family consists of four generations with 52 members. Ten members of the family are affected by stenosis or occlusion of portal and hepatic veins as well as lymphatic vessels, formation of collateral circulation, and pulmonary valve stenosis. Numbers in parentheses denote the age at the diagnosis of MOVLD.

III-16, and IV-10 were diagnosed at the ages of 16, 14, and 5, respectively; and all of the rest were diagnosed in adulthood. Based on the International Society for the Study of Vascular Anomalies (ISSVA) classification, these malformations belong to the "anomalies of major named vessels" and are different from any reported vascular malformations[10]; therefore, we named this syndrome "multiorgan venous and lymphatic defect" (or MOVLD). Detailed clinical information on affected family members is presented in Table 1.

To be specific, the proband (III-15) and family members II-4, II-6, II-10, III-12, and III-16 had refractory chylothorax caused by thoracic duct obliteration confirmed by lymphangiogram and/or clinical evaluation; and II-4 and III-16 died of respiratory failure related to chylothorax at 45 and 16 years old, respectively. II-4, III-13, and IV-10 had pulmonary valve stenosis (which is classified as a type of "named vessel anomalies" in the ISSVA classification 2018)[10]; and II-10, III-12, and III-15 had mild pericardial effusion. The nature of the effusion was unknown as aspiration was not performed. In addition, II-10 and III-15 had ascites. Splenomegaly and esophageal varication were observed in all affected family members except III-15 and III-13. III-8, III-12, and III-15 had fundus varication. III-8 had a gastrorenal shunt, and II-6 had a portal venous aneurysm. None of the family members had a history of gastrointestinal bleeding. Detailed clinical investigation ruled out all of the known causes of these symptoms, such as hepatitis, autoimmune diseases, vasculitis, coagulation disorders, or history of abdominal surgery and trauma. Liver biopsy showed no abnormal morphological change. Because the phenotypes seemed to be inherited in an autosomal dominant fashion, we performed genetic analysis.

DEAD-BOX HELICASE 24 MUTATION P.GLU271LYS WAS ASSOCIATED WITH MOVLD

To determine the genetic basis of MOVLD, we first performed chromosomal microarray analysis using samples of family members II-10 and II-12, who were affected, and II-8 and II-12, who had been definitively shown to be unaffected. This analysis did not identify any gains or losses of whole chromosomes or portions of chromosomes in the affected cases from the family (data not shown), suggesting that a small sequence variant(s), rather than large-scale genomic anomalies, may be responsible for the clinical phenotypes observed.

Next, genomic DNA from 16 adults from the second and third generations of the family was used for linkage analysis to ascertain small genetic variants. Linkage analysis identified three loci with ExLOD score >3.0: *1q44* (ExLOD = 3.46, at 275 cM), *2q36.1* (ExLOD = 3.28, at 225 cM), and *14q32.12* (ExLOD = 3.59, at 96 cM) (Fig. 3A; Supporting Fig. S8).

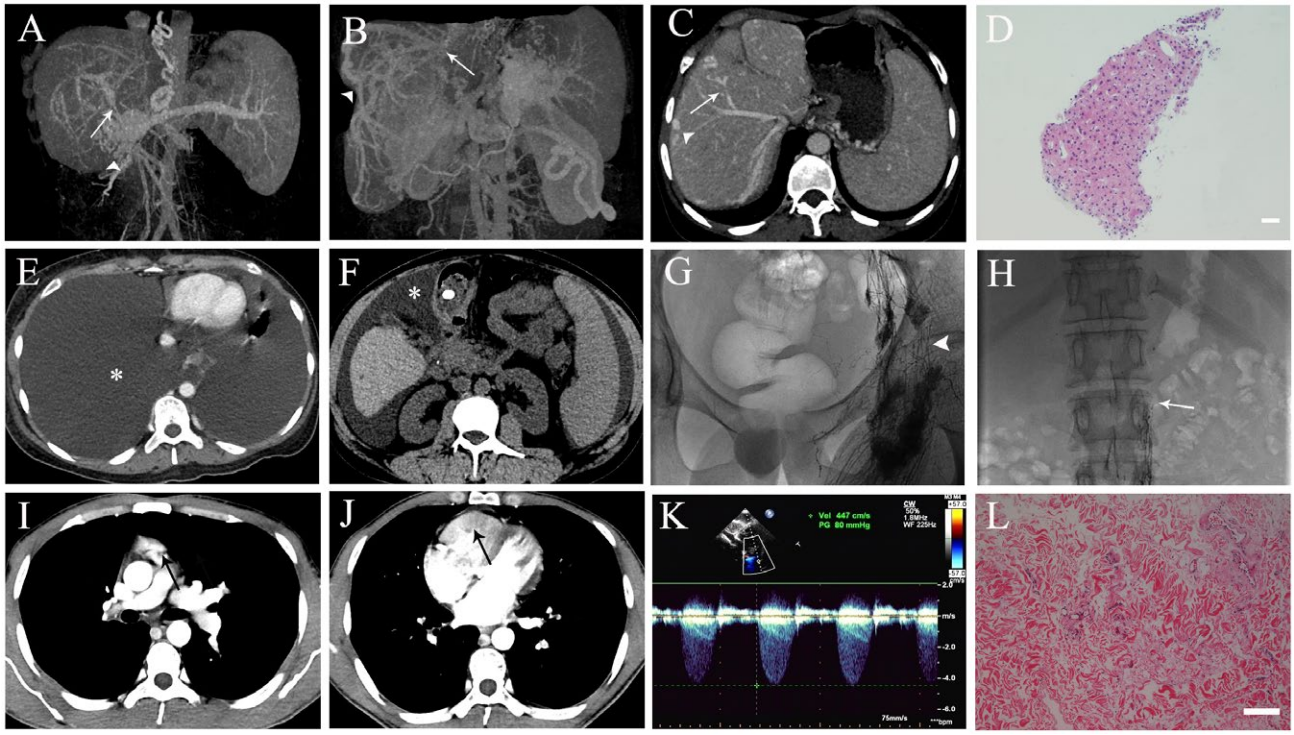

FIG. 2. Clinical and histological features of the patients in the MOVLD syndrome family. (A-C) Three-dimensional construction of abdominal CT shows stenosis of the portal vein (A; white arrow) in patient II-6 and hepatic vein stenosis (B,C; white arrow) in patient III-12 with formation of collateral circulation (white arrowhead). (D) Liver tissue specimens from patient II-6 are normal by light microscopy. Hematoxylin and eosin stain; scale bar, 100 μm. (E) Chest CT shows a large amount of pleural effusion (white asterisk) in patient III-15. (F) Mild ascites (asterisk) is observed on the abdominal CT in patient II-10. (G,H) Lymphangiography shows thoracic duct obliteration (white arrow) and formation of collateral circulation (white arrowhead) in patient III-16. (I,J) Enhanced CT imaging shows thickening of the pulmonary valve (I; black arrow) and myocardial hypertrophy (J; black arrow) in patient III-13. (K,L) In patient III-13, color Doppler ultrasound of the heart shows pulmonary valve stenosis (K) and hematoxylin and eosin staining shows intimal hyperplasia of the pulmonary valve by light microscopy (L; scale bar, 200 μm).

Haplotype analysis using SNP data for the three loci showed that the only haplotype shared by all affected family members was that flanked by markers rs4900162 and rs8006174 on chromosome *14q32.12*, which also had the highest ExLOD Score (Fig. 3B). This haplotype was not found in any unaffected members available for genetic testing except one, III-18. The presence of the haplotype in the 13-year-old, III-18, which is absent for any identified phenotype in the MOVLD family, may be explained by the late onset of the disease or incomplete penetrance. The other two candidate loci identified by linkage analysis were excluded by haplotype segregation. These results demonstrated that the disease segregated with a haplotype on chromosome *14q32.12*.

To identify the gene(s) underlying MOVLD, exome sequencing was performed in 2 affected individuals (III-8 and III-10) and 2 definitely unaffected individuals (II-8 and II-12) of the family. This revealed 35 potentially deleterious variations (predicted by PolyPhen-2[34], https://genetics.bwh.harvard.edu/pph2/) in 23 genes exome-wide after excluding the variations shared between the affected and the unaffected members. Among these, p.Glu271Lys (rs149296999) in DEAD-box helicase 24 (*DDX24*) (Fig. 3C) was the only mutation also identified in the linked and cosegregated haplotype. This mutation replaces an acidic glutamine residue with an alkaline lysine residue and is classified as "probably pathogenic" by the ACMG guidelines.

Furthermore, the p.Glu271Lys mutation was not found in 100 people sequenced who underwent clinical and imaging examinations and appeared normal (data not shown). Together, these results suggested that this

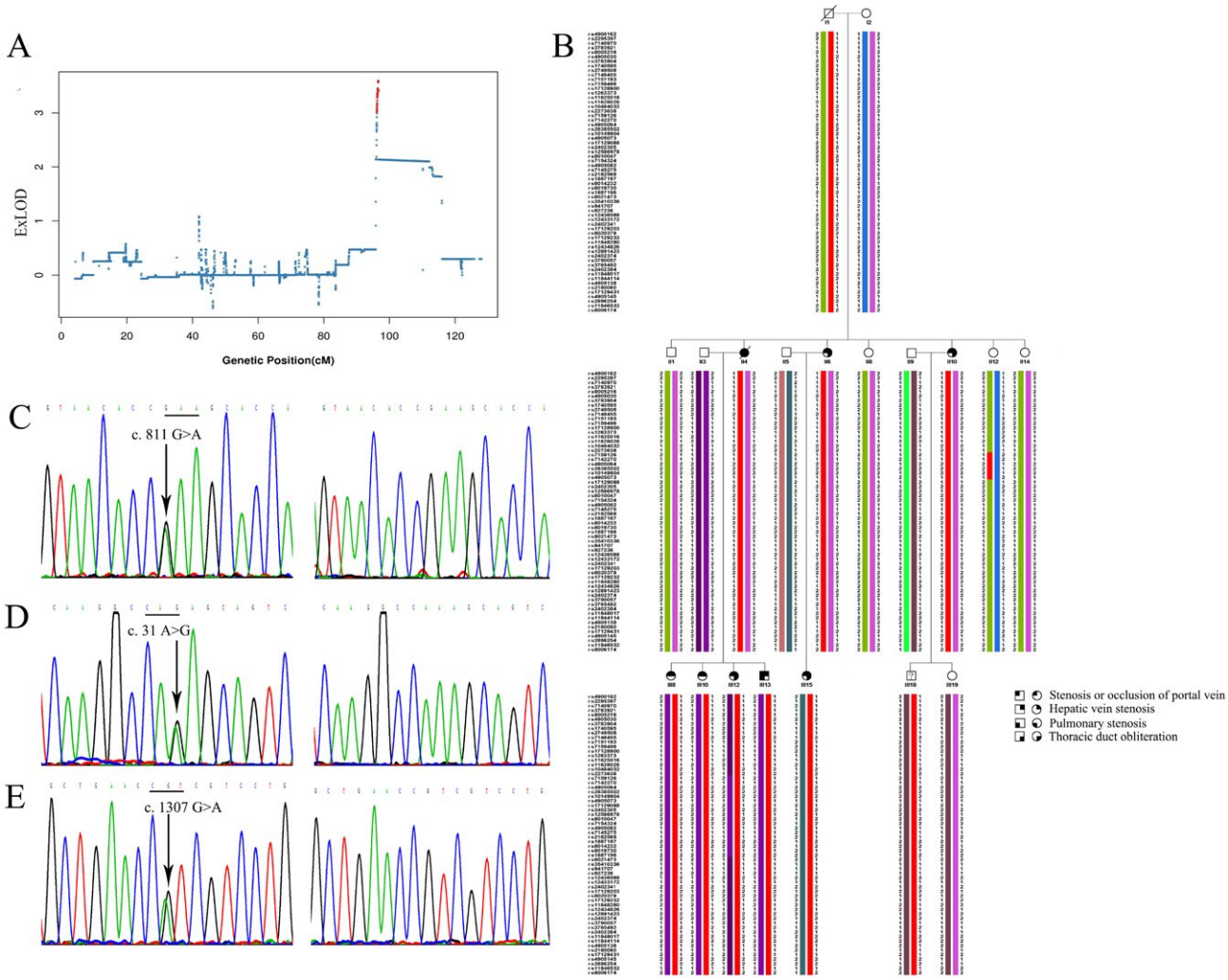

FIG. 3. *DDX24* mutations in patients with MOVLD syndrome and sporadic patients. (A) Multipoint parametric linkage analysis of the MOVLD family revealed the most significant linkage (ExLOD score = 3.59) in the region of 96 cM on chromosome 14. (B) Haplotype reconstruction for the MOVLD family with segregation of the disease allele (shown in red) in all affected family members from the first to the third generation. (C-E) Partial DNA sequences of *DDX24* are shown. Bottom panels show the wild-type *DDX24* sequences, and top panels show the mutations identified in the MOVLD family and, later, in some patients with sporadic disease of similar phenotype: c.811G>A (p.Glu271Lys) (C), c.31A>G (p.Lys11Glu) (D), c.1307G>A (p.Arg436His) (E).

mutation in *DDX24*, which encodes an uncharacterized RNA helicase, could be involved in MOVLD.

DDX24 MUTATIONS WERE ALSO IDENTIFIED IN SPORADIC PATIENTS WITH VASCULAR MALFORMATIONS

To investigate the involvement of *DDX24* in vascular malformations of similar phenotype, we recruited 10 unrelated patients exhibiting sporadic portal vein stenosis or occlusion with formation of collateral circulation as well as 151 idiopathic BCS patients characterized by stenosis or occlusion of the hepatic vein and/or inferior vena cava in whom all of the known causes were excluded (see above, Sporadic Patient Recruitment) and searched for *DDX24* mutations in these cases using Sanger sequencing (Table 1).[35,36] Intriguingly, the p.Glu271Lys (rs149296999) mutation found in our

MOVLD family was identified in 1 of the 10 sporadic cases screened and 14 cases from the cohort of 151 idiopathic BCS patients.

We also identified two additional *DDX24* mutations that are classified as "damaging or probably damaging" by the ACMG guidelines in the 151 BCS patients: a p.Lys11Glu mutation (rs142609376) (Fig. 3D) found in 10 BCS cases and a p.Arg436His mutation (Fig. 3E) in 1 BCS case. All of the mutations identified in the patients occurred in evolutionarily conserved sequences of *DDX24* (Supporting Fig. S9), suggesting that the mutation-affected regions are likely to be indispensable to the function of this gene.

PROTEIN STRUCTURAL MODELING

The DDX24 protein is predicted to contain two domains: a helicase adenosine triphosphate (ATP)–binding domain (also called the N-terminal domain in homologous proteins, residues 192-532) and a C-terminal domain (residues 578-723).[37] Residues Glu271 and Arg436 are located in the predicted ATP-binding domain (Fig. 4A). To determine the possible effect of these two mutations on protein functions, we built a structural model for this domain of DDX24 using the N-terminal domain of HERA (PDB 2GXQ) because it is the closest homology model (Fig. 4B).

Alignment of the above sequences revealed that the ATP-binding domain of DDX24 contains an insertion sequence comprising residues 257-385, which includes one of the mutated residues, Glu271 (Fig. 4C). Therefore, we were unable to model the structure of this region or to predict the effect of the mutated residue on the protein function.

The other mutated residue, Arg436, is within the aligned structure. In particular, it is located on the α5 helix, exposed to solvent, and does not form significant interactions with the nearby residues (Fig. 4B). Although the p.Arg436His mutation is unlikely to affect the overall structure of the ATP-binding domain of DDX24 based on the modeled structure, it is possible that the basic residue Arg436 may interact with and stabilize the insertion region of the ATP-binding domain of DDX24, which is in close proximity to the α5 helix and contains many negatively charged residues. Interestingly, in addition to Arg436, the α5 helix contains the basic residues Lys429, Arg432, and Arg437, which produce a positively charged region and thus may be involved in the interaction with a negatively charged partner molecule (such as a protein region or RNA).

Unfortunately, we were unable to predict whether the p.Lys11Glu mutation disrupts the structure or function of DDX24 because there is no homologous structure to the N-terminal region of DDX24 in PDB.

DDX24 KNOCKDOWN PROMOTES CELL MIGRATION AND TUBE FORMATION IN ENDOTHELIAL CELLS

Genetic knockout of *DDX24* has been reported to cause embryonic lethality, and its function has been related to innate immune signaling.[38] However, no studies have suggested a role of *DDX24* in vascular diseases. Therefore, to assess the function of *DDX24* in endothelium, we performed siRNA-mediated gene knockdown in several human primary endothelial cells, including HUVECs, HLECs, HHSECs, and immortalized HUVECs (Supporting Figs. S10 and S11A). Although siRNA treatment did not affect the growth of HUVECs (Supporting Fig. S11B), cell migration and tube formation were significantly enhanced upon *DDX24* knockdown (Fig. 5A; Supporting Fig. S11C,D). We also observed increased cell migration in siRNA-treated HLECs and HHSECs (Fig. 5B,C).

To better understand the function of *DDX24*, we performed gene expression analysis using RNA sequencing. We found 144 genes up-regulated and 227 genes down-regulated in HUVECs treated with *DDX24* siRNA compared with scrambled

FIG. 4. Homology modeling and sequence alignment of DDX24. (A) Schematic representation of DDX24 showing the predicted ATP-binding and C-terminal domains. The positions of the three amino acid changes found in the MOVLD family and the sporadic patients with disease of a similar phenotype are also shown. (B) Homology modeling of the ATP-binding domain of DDX24 based on the structure of the ATP-binding domain of the homologous protein HERA. Dashed line denotes the inserted region. The basic residues of the α5 helix in DDX24 are noted. (C) Sequence alignment of the ATP-binding domain of DDX24 with the N-terminal domain of HERA. Aligned sequences are highlighted in red blocks; insertion region is in green box; mutations identified in patients are indicated by blue arrows.

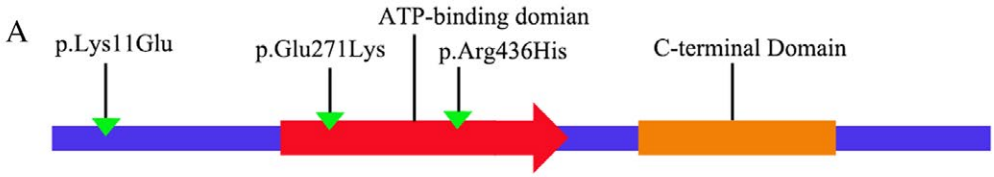
A
p.Lys11Glu
p.Glu271Lys
ATP-binding domian
p.Arg436His
C-terminal Domain

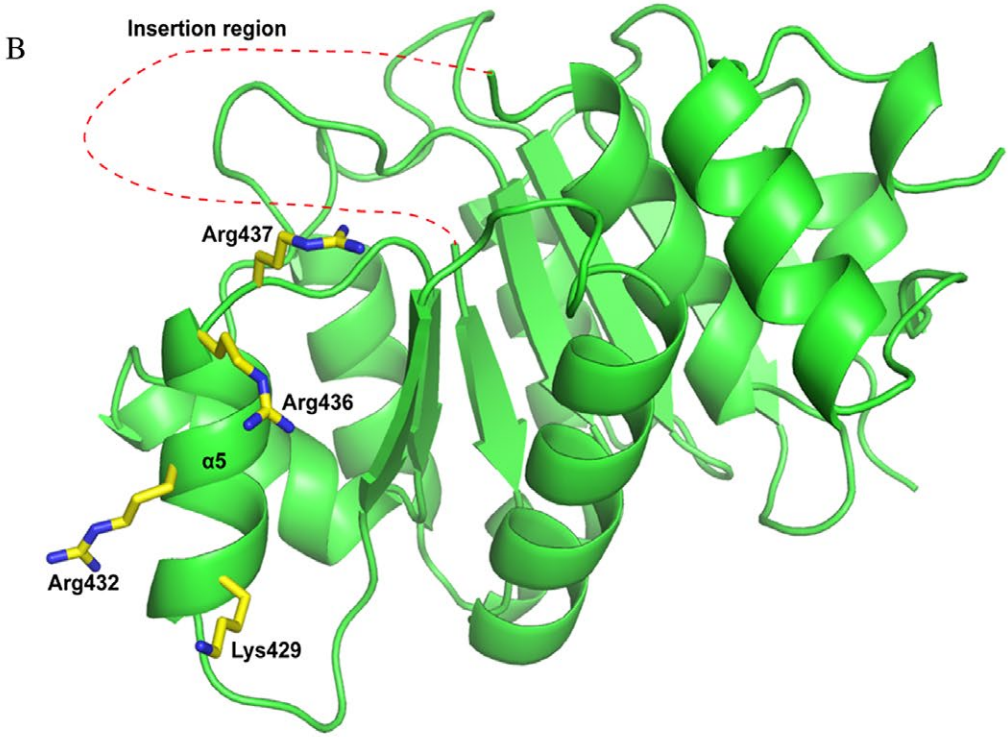
B
Insertion region
Arg437
Arg436
α5
Arg432
Lys429

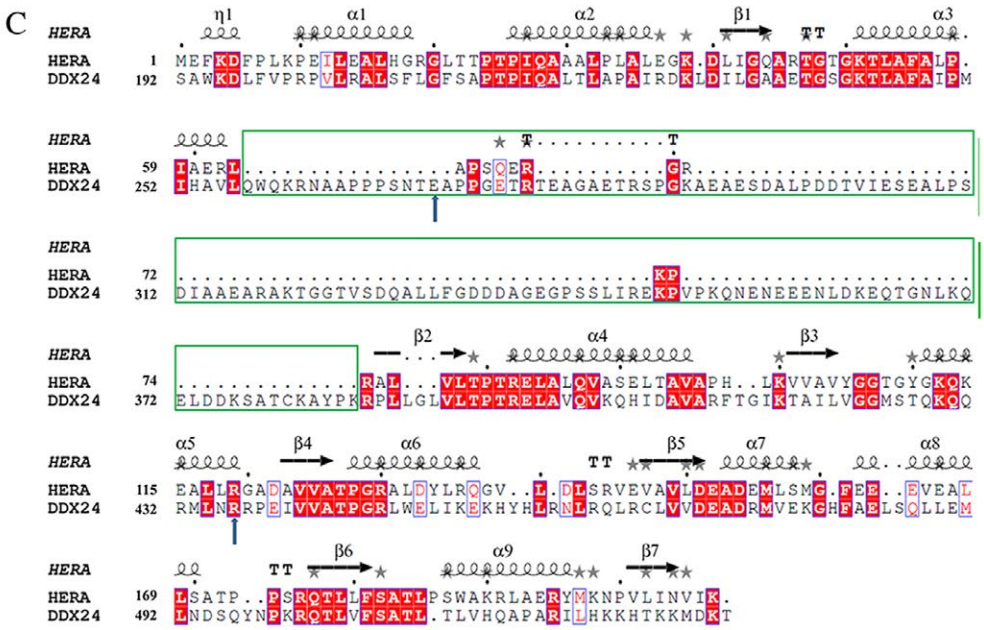
C
HERA
HERA 1 MEFKDFPLKPELEALHGRGLTTPTPIQAAALPLALEGK.DLIGQARTGTGKTLAFALP.
DDX24 192 SAWKDLFVPRPVLRALSFLGFSAPTPIQALTLAPAIRDKLDILGAAETGSGKTLAFAIPM
HERA 59 IAERL.....APSQER.....GR.....
DDX24 252 IHAVLQWQKRNAAPPPSNTEAPPGETRTEAGAETRSPGKAEAESDALPDDTVIESEALPS
HERA 72 .....KP.....
DDX24 312 DIAAEARAKTGGTVSDQALLFGDDDAGEGPSSLIREKPVPKQNENEEENLDKEQTGNLKQ
HERA 74 .....RALVLTPTRELALQVASELTAVAPH..LKVVAVYGGTGYGKQK
DDX24 372 ELDDKSATCKAYPKRPLLGLVLTPTRELAVQVKQHIDAVARFTGIKTAILVGGMSTQKQQ
HERA 115 EALLRGADAVVATPGRALDYLRQGV..LDLSRVEVAVLDEADEMLSMGFEE..EVEAL
DDX24 432 RMLNRRPEIVVATPGRLWELIKEKHYHLRNLRQLRCLVVDEADRMVEKGHFAELSQLLEM
HERA 169 LSATP..PSRQTLLFSATLPSWAKRLAERYMKNPVLINVIK.
DDX24 492 LNDSQYNPKRQTLVFSATL.TLVHQAPARILHKKHTKKMDKT

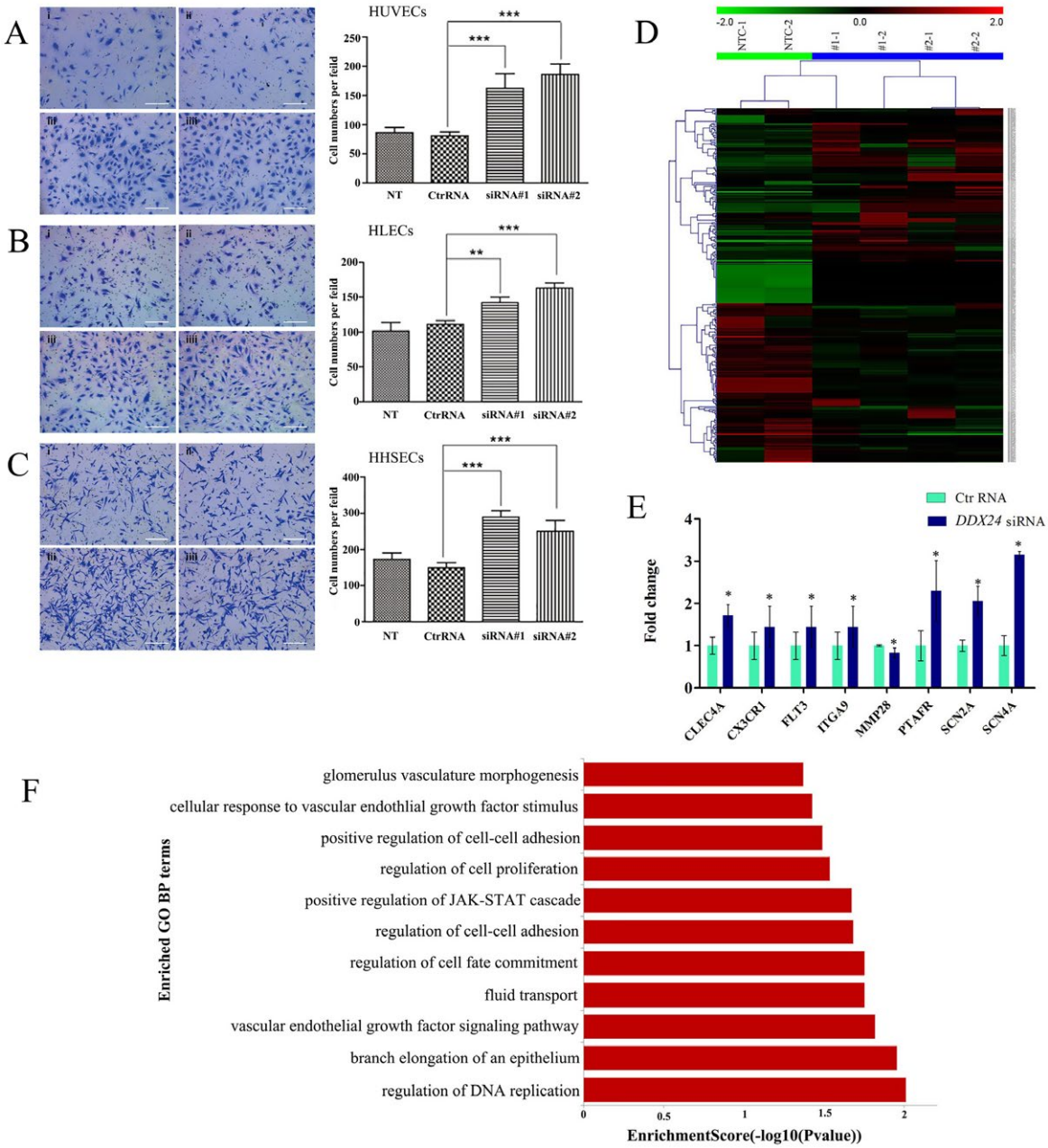

FIG. 5. Effects of siRNA-mediated knockdown of *DDX24* in human endothelial cells. (A-C) Migration of HUVECs (A), HLECs (B), and HHSECs (C) was quantified using a modified Boyden chamber (scale bar, 100 μm): (i) no treatment, (ii) scrambled siRNA, (iii) *DDX24* siRNA #1, (iv) *DDX24* siRNA #2. The data are presented as the mean cell number ± SD per field of view (n = 6; $^{***}P$ <0.001). Each individual experiment was repeated at least three times. (D) siRNA-treated immortalized HUVECs were analyzed by RNA-sequencing analysis. Up-regulated and down-regulated genes are shown in the heat map. Log2 relative gene expression is visualized as shades of red (higher than treatment with scrambled siRNA) and shades of green (lower than treatment with scrambled siRNA). (E) Genes validated by reverse-transcription real-time quantitative PCR, including the cell migration genes *CX3CR1* and *PTAFR*, which were significantly up-regulated in the *DDX24* siRNA-treated HUVECs. Ctr RNA denotes scrambled siRNA ($^{*}P$ <0.05). (F) Gene ontology analysis was performed to assess biological pathways enriched among the differentially expressed genes by *DDX24* knockdown. Abbreviations: BP, biological pathway; CLEC4A, C-type lectin domain family 4 member A; Ctr, control; FLT3, Fms-related tyrosine kinase 3; GO, gene ontology; ITGA9, integrin subunit alpha 9; JAK-STAT, Janus kinase–signal transducer and activator of transcription; MMP28, matrix metallopeptidase 28; NT, no treatment; NTC, scramble siRNA-treated; SCN2A/SCN4A, sodium voltage-gated channel alpha subunits 2/4; #1 and #2, two different siRNAs treated.

siRNA-treated HUVECs (Fig. 5D). These findings were validated by real-time quantitative PCR (Fig. 5E), including the genes involved in cell migration, C-X3-C motif chemokine receptor 1 (*CX3CR1*) and platelet-activating factor receptor (*PTAFR*), which were significantly up-regulated in the *DDX24* siRNA-treated HUVECs. Gene ontology analysis revealed that genes involved in the vascular endothelial growth factor (VEGF) signaling pathway and in cell migration (Fig. 5F) were enriched in *DDX24*-knockdown cells. In sum, these results suggest that DDX24 acts as a suppressor in endothelial cell migration and angiogenesis.

Discussion

To identify mutations associated with malformations of vessels to the viscera, we focused on the study of a large family with a syndrome involving vascular malformations in multiple organs, with stenosis or occlusion of portal and hepatic veins being the most prominent. Using linkage and haplotype analyses, we linked this syndrome to a single locus on chromosome *14q32.12* where a heterozygous missense mutation in *DDX24* segregated with the disease. Furthermore, we identified this mutation and two other mutations in *DDX24* in a number of patients with sporadic stenosis or occlusion of portal and hepatic veins and/or inferior vena cava. Functional analysis in endothelial cells related this gene to VEGF signaling and cell migration pathways.

MOVLD is a unique syndrome with distinctive clinical characteristics. First of all, patients with MOVLD syndrome display vascular malformations involving multiple major named vessels with anomalies in number, diameter, and/or valves, according to the ISSVA classification.[10] Second, stenosis or occlusion of portal and hepatic veins in other vascular malformations often causes noncirrhotic portal hypertension.[39] However, complications of portal hypertension did not occur in the affected MOVLD family members. Instead, respiratory failure resulting from refractory chylothorax was the main cause of death for the 2 affected members (II-4 and III-16). As a matter of fact, the proband was also admitted to the hospital as a result of respiratory distress. We recommend using enhanced CT for the diagnosis of MOVLD for more objective and accurate detection. In terms of treating chylothorax, thoracic duct embolization or ligation has been reported to treat patients with chylous leaks.[40] However, we did not observe lymphatic vessel dilation or chylous leaks in the MOVLD patients; therefore, thoracic duct embolization or ligation might not be optimal. In this case, sirolimus therapy might be an option.[41]

To unravel the genetic basis for MOVLD syndrome, we identified the p.Glu271Lys mutation of *DDX24* by two different genetic approaches. Linkage analysis linked all of the affected family members to *14q32.12* and haplotype analysis narrowed down the location of the causative region to a 1.16-cM candidate interval. Exome sequencing analysis revealed that only p.Glu271Lys in *DDX24* was located in the cosegregated, disease gene–bearing haplotype and within the candidate interval. Moreover, the p.Glu271Lys mutation was not found in 100 unaffected people who were randomly chosen. These results indicated that the *DDX24* p.Glu271Lys mutation was causatively associated with the MOVLD syndrome.

Notably, the Exac database (https://exac.broadinstitute.org/) and the 1000 Genomes Project (https://www.internationalgenome.org/) show that the frequency of *DDX24* p.Glu271Lys in the Asian population is approximately 1%. This seems to be discordant with the lower incidence of the visceral vascular malformations. However, the fact is that there have been no reliable data regarding the incidence of visceral vascular malformations as the insidious disease onset and the diagnosis often rely on careful imaging examinations before severe complications appear. It is possible that patients with this type of vascular malformation were enrolled into the Exac database and that the prevalence of such diseases is much higher than current estimates. Furthermore, the potential incomplete penetrance/late onset may also suggest a discordance between the frequency of the mutation and the low prevalence in the general population, which can be exemplified by III-18 in the MOVLD family who carried the mutation but was unaffected by all known measures at the age of 13 years. Therefore, individuals with this mutation may require careful and detailed clinical and imaging examinations to determine whether malformations of vessels to the viscera are present, particularly given the known insidious onset and deep location of the disease. Similar to other types of vascular malformations, it is difficult to determine the onset age of MOVLD syndrome. In

addition, the level of the penetrance and the degree to which a certain gene contributes to the disease are variable.[42] The above-mentioned factors may explain why subject III-18 shared the haplotype but did not display any symptoms.

In the 161 patients with sporadic disease of similar vascular phenotype, we found the following three *DDX24* mutations in a total of 26 cases: p.Glu271Lys (rs149296999) mutation in 15 cases, p.Lys11Glu (rs142609376) mutation in 10 cases, and p.Arg436His mutation in 1 case. The high frequency of *DDX24* mutations among these patients implies an essential role for DDX24 in vascular malformations. Because the same gene was mutated in both the MOVLD family and idiopathic BCS, the defect of DDX24 may underlie multiple types of vascular malformations with similar phenotypes.

DDX24, a member of the DEAD-box protein family, belongs to a large group of putative RNA helicases that mediate the nucleoside triphosphate–dependent unwinding of double-stranded RNA.[43] Few studies regarding DDX24 have been reported, and the function of DDX24 has been mainly studied in the context of oncology.[44] Thus far, no studies on DDX24 in vascular diseases have been reported. Our findings suggest that DDX24 is not involved in endothelial cell growth, which agrees with a previous report stating that depletion of DDX24 inhibits the growth of tumor cell lines but not normal cells.[44] Because *DDX24* mutations impaired venous and lymphatic functions in patients, we performed cell functional assays in HUVECs, HLECs, and HHSECs and found that *DDX24* knockdown promoted endothelial cell migration and tube formation. Correspondingly, gene expression analysis revealed that genes involved in cell migration, such as *CX3CR1* and *PTAFR*, were up-regulated in cells lacking DDX24. Our findings provide a link between *DDX24* and malformation of the portal and hepatic veins, lymphatic vessels, and pulmonary valve and indicate a crucial role for DDX24 in endothelial cell functions. However, the molecular mechanism of how DDX24 is involved in vascular malformation remains to be further investigated.

During development, endocardial cells form a primitive vascular plexus surrounding the liver bud and subsequently contribute to a substantial portion of the liver vasculature. Moreover, the endocardium of the sinus venosus is a source for the hepatic plexus.[45] These anatomical connections may explain the combined liver, lymphatic, and heart vascular malformations in the affected family members and in some cases of BCS. Mutant DDX24 may affect normal development by interfering with either the unwinding of RNA or other factors involved in these processes. DDX24 may thus function as a negative regulator in endothelial cell migration and tube formation as well as a key regulator for normal vascular development in the liver, lymphatic system, and heart. The fact that DDX24 acts as a negative regulator in innate immune gene regulation echoes our findings.[38]

Identification of the genetic basis of the family with MOVLD and a subset of patients with sporadic disease of similar phenotype revealed a key role of *DDX24* in vascular malformations. The function of DDX24 in vascular development is currently being investigated in animal models such as single nucleotide–mutated zebrafish and conditional knockout mice. Detailed signaling pathways are to be determined in order to develop therapeutic targets for this protein. These findings will allow genetic diagnosis and treatment for *DDX24*-related vascular malformations.

REFERENCES

1) Eifert S, Villavicencio JL, Kao TC, Taute BM, Rich NM. Prevalence of deep venous anomalies in congenital vascular malformations of venous predominance. J Vasc Surg 2000;31:462-471.
2) Wassef M, Blei F, Adams D, Alomari A, Baselga E, Berenstein A, et al. Vascular anomalies classification: recommendations from the International Society for the Study of Vascular Anomalies. Pediatrics 2015;136:e203-e214.
3) Greene AK. Vascular anomalies: current overview of the field. Clin Plast Surg 2011;38:1-5.
4) Ernemann U, Kramer U, Miller S, Bisdas S, Rebmann H, Breuninger H, et al. Current concepts in the classification, diagnosis and treatment of vascular anomalies. Eur J Radiol 2010;75:2-11.
5) Davenport M. Congenital vascular malformations of the liver: an association with trisomy 21. J Pediatr Gastroenterol Nutr 2017;64:e82.
6) Bowen JM, Connolly HM. Of Marfan's syndrome, mice, and medications. N Engl J Med 2014;371:2127-2128.
7) Boon LM, Mulliken JB, Vikkula M, Watkins H, Seidman J, Olsen BR, et al. Assignment of a locus for dominantly inherited venous malformations to chromosome 9p. Hum Mol Genet 1994;3:1583-1587.
8) Brouillard P, Vikkula M. Genetic causes of vascular malformations. Hum Mol Genet 2007;16:R140-R149.
9) Queisser A, Boon LM, Vikkula M. Etiology and genetics of congenital vascular lesions. Otolaryngol Clin North Am 2018;51:41-53.
10) International Society for the Study of Vascular Anomalies. ISSVA classification for vascular anomalies. https://www.issva.org/UserFiles/file/ISSVA-Classification-2018.pdf. Published May 2018.

11) Greene AK, Goss JA. Vascular anomalies: from a clinicohistologic to a genetic framework. Plast Reconstr Surg 2018;141:709e-717e.
12) **Wouters V**, **Limaye N**, Uebelhoer M, Irrthum A, Boon LM, Mulliken JB, et al. Hereditary cutaneomucosal venous malformations are caused by TIE2 mutations with widely variable hyper-phosphorylating effects. Eur J Hum Genet 2010;18:414-420.
13) Brouillard P, Boon LM, Mulliken JB, Enjolras O, Ghassibe M, Warman ML, et al. Mutations in a novel factor, glomulin, are responsible for glomuvenous malformations ("glomangiomas"). Am J Hum Genet 2002;70:866-874.
14) **Gordon K**, **Schulte D**, Brice G, Simpson MA, Roukens MG, van Impel A, et al. Mutation in vascular endothelial growth factor-C, a ligand for vascular endothelial growth factor receptor-3, is associated with autosomal dominant Milroy-like primary lymphedema. Circ Res 2013;112:956-960.
15) Boon LM, Mulliken JB, Vikkula M. RASA1: variable phenotype with capillary and arteriovenous malformations. Curr Opin Genet Dev 2005;15:265-269.
16) Denier C, Labauge P, Bergametti F, Marchelli F, Riant F, Arnoult M, et al. Genotype–phenotype correlations in cerebral cavernous malformations patients. Ann Neurol 2006;60:550-556.
17) Yu J, Streicher JL, Medne L, Krantz ID, Yan AC. EPHB4 mutation implicated in capillary malformation-arteriovenous malformation syndrome: a case report. Pediatr Dermatol 2017;34:e227-e230.
18) **Amyere M**, **Revencu N**, Helaers R, Pairet E, Baselga E, Cordisco M, et al. Germline loss-of-function mutations in EPHB4 cause a second form of capillary malformation-arteriovenous malformation (CM-AVM2) deregulating RAS-MAPK signaling. Circulation 2017;136:1037-1048.
19) Menon KV, Shah V, Kamath PS. The Budd-Chiari syndrome. N Engl J Med 2004;350:578-585.
20) Plessier A, Rautou PE, Valla DC. Management of hepatic vascular diseases. J Hepatol 2012;56(Suppl. 1):S25-S38.
21) Abecasis GR, Cherny SS, Cookson WO, Cardon LR. Merlin—rapid analysis of dense genetic maps using sparse gene flow trees. Nat Genet 2002;30:97-101.
22) Thiele H, Nurnberg P. HaploPainter: a tool for drawing pedigrees with complex haplotypes. Bioinformatics 2005;21:1730-1732.
23) Li H, Durbin R. Fast and accurate short read alignment with Burrows-Wheeler transform. Bioinformatics 2009;25: 1754-1760.
24) **Li H**, **Handsaker B**, Wysoker A, Fennell T, Ruan J, Homer N, et al. The Sequence Alignment/Map format and SAMtools. Bioinformatics 2009;25:2078-2079.
25) Wang K, Li M, Hakonarson H. ANNOVAR: functional annotation of genetic variants from high-throughput sequencing data. Nucleic Acids Res 2010;38:e164.
26) Amendola LM, Jarvik GP, Leo MC, McLaughlin HM, Akkari Y, Amaral MD, et al. Performance of ACMG-AMP variant-interpretation guidelines among nine laboratories in the Clinical Sequencing Exploratory Research Consortium. Am J Hum Genet 2016;98:1067-1076.
27) Martin-Llahi M, Albillos A, Banares R, Berzigotti A, Garcia-Criado MA, Genesca J, et al. Vascular diseases of the liver. Clinical guidelines from the Catalan Society of Digestology and the Spanish Association for the Study of the Liver. Gastroenterol Hepatol 2017;40:538-580.
28) Valla DC. Primary Budd-Chiari syndrome. J Hepatol 2009; 50:195-203.
29) Liu L, Qi XS, Zhao Y, Chen H, Meng XC, Han GH. Budd-Chiari syndrome: current perspectives and controversies. Eur Rev Med Pharmacol Sci 2016;20:3273-3281.
30) Rzechorzek NJ, Blackwood JK, Bray SM, Maman JD, Pellegrini L, Robinson NP. Structure of the hexameric HerA ATPase reveals a mechanism of translocation-coupled DNA-end processing in archaea. Nat Commun 2014;5:5506.
31) Eswar N, Eramian D, Webb B, Shen MY, Sali A. Protein structure modeling with MODELLER. Methods Mol Biol 2008;426:145-159.
32) Justus CR, Leffler N, Ruiz-Echevarria M, Yang LV. *In vitro* cell migration and invasion assays. J Vis Exp 2014;88:51046.
33) DeCicco-Skinner KL, Henry GH, Cataisson C, Tabib T, Gwilliam JC, Watson NJ, et al. Endothelial cell tube formation assay for the *in vitro* study of angiogenesis. J Vis Exp 2014;91:51312.
34) PolyPhen-2. Home fact sheet. http://genetics.bwh.harvard.edu/pph2/. Published December 9, 2010. Accessed February 2012.
35) Gallego C, Velasco M, Marcuello P, Tejedor D, De Campo L, Friera A. Congenital and acquired anomalies of the portal venous system. Radiographics 2002;22:141-159.
36) European Association for the Study of the Liver. EASL clinical practice guidelines: vascular diseases of the liver. J Hepatol 2016;64:179-202.
37) Zhao Y, Yu L, Fu Q, Chen W, Jiang J, Gao J, et al. Cloning and characterization of human DDX24 and mouse Ddx24, two novel putative DEAD-Box proteins, and mapping DDX24 to human chromosome 14q32. Genomics 2000;67:351-355.
38) Ma Z, Moore R, Xu X, Barber GN. DDX24 negatively regulates cytosolic RNA-mediated innate immune signaling. PLoS Pathog 2013;9:e1003721.
39) DeLeve LD, Valla DC, Garcia-Tsao G. American Association for the Study of Liver Diseases. Vascular disorders of the liver. Hepatology 2009;49:1729-1764.
40) Chen E, Itkin M. Thoracic duct embolization for chylous leaks. Semin Intervent Radiol 2011;28:63-74.
41) Harari S, Elia D, Torre O, Bulgheroni E, Provasi E, Moss J. Sirolimus therapy for patients with lymphangioleiomyomatosis leads to loss of chylous ascites and circulating LAM cells. Chest 2016;150:e29-e32.
42) de Vos IJ, Vreeburg M, Koek GH, van Steensel MA. Review of familial cerebral cavernous malformations and report of seven additional families. Am J Med Genet A 2017;173:338-351.
43) Yamauchi T, Nishiyama M, Moroishi T, Yumimoto K, Nakayama KI. MDM2 mediates nonproteolytic polyubiquitylation of the DEAD-Box RNA helicase DDX24. Mol Cell Biol 2014;34:3321-3340.
44) Shi D, Dai C, Qin J, Gu W. Negative regulation of the p300–p53 interplay by DDX24. Oncogene 2016;35:528-536.
45) Zhang H, Pu W, Tian X, Huang X, He L, Liu Q, et al. Genetic lineage tracing identifies endocardial origin of liver vasculature. Nat Genet 2016;48:537-543.

Author names in bold designate shared co-first authorship.

Supporting Information

Additional Supporting Information may be found at onlinelibrary.wiley.com/doi/10.1002/hep.30200/suppinfo.